

Error cancellation modeling and its application to machining process control

HUI WANG and QIANG HUANG*

Department of Industrial and Management Systems Engineering, University of South Florida, Tampa, FL 33620, USA
E-mail: huangq@eng.usf.edu

Received and accepted

The product quality in a machining process can be affected by datum surface imperfections, fixture locator errors, and machine tool errors. It has been previously observed that these effects can cancel out one another for certain features. The mathematical modeling and analysis of this phenomenon is currently an open issue. We use the concept of an Equivalent Fixture Error (EFE) embedded into a modeling methodology to obtain insights into this fundamental phenomenon and achieve an improved process control. Based on our process fault model we develop a sequential root-cause identification procedure and EFE compensation methodology. A case study is presented to demonstrate the proposed diagnostic procedure. A simulation study is also performed to illustrate the error compensation procedure.

1. Introduction

In a machining process, product quality is mainly affected by fixture, datum, and machine tool errors. A fixture is a device used to locate, clamp, and support a workpiece during machining, assembly, or inspection. A fixture error is considered to be a significant fixture deviation of a locator from its specified position. Machining datum are those part features that are in direct contact with the fixture locators. Datum error is deemed to be the significant deviation of datum surfaces and is mainly induced by imperfections in raw workpieces or faulty operations in previous stages. Together the fixture and datum surfaces provide a reference system for accurate cutting operations using machine tools. Machine tool error is modeled in terms of significant tool path deviations from its intended route. In this paper, we mainly focus on kinematic aspects of these three error types.

It has been widely noted that fixture, datum, and machine tool errors may cancel out one another, i.e., their combined effect will reduce deviations in part features. This phenomenon may have the drawback that it is possible for it to conceal the fact that multiple errors have occurred in the process, however, there is the opportunity for us to purposely use one type of error to counteract or compensate another error and thereby reduce variation.

To our knowledge, no study has been performed that models and explores this cancellation effect among different types of error sources in order to create quality control in

machining processes. Most research has been focused on fixture design and machine tool error modeling.

Fixture error is generally considered to be one of the crucial factors in optimal fixture design and analysis. Shawki and Abdel-Aal (1965) experimentally studied the impact of fixture wear on the positional accuracy of a workpiece. Asada and By (1985) performed the kinematic modeling, analysis, and characterization of adaptable fixturing. Screw theory was developed as an attempt to estimate locating accuracy under a rigid body assumption (Ohwovoriole and Roth, 1981; Ball, 1990). Weill *et al.* (1991) have developed several optimization approaches to minimize workpiece positioning errors. A robust fixture design was proposed by Cai *et al.* (1997) that was able to minimize positional errors. Marin and Ferreira (2003) analyzed the influence of dimensional locator errors on the tolerance allocation problem. Researchers have also considered the effect of the geometry of the datum surface on the fixture design. The optimization of the locating setup proposed by Weill *et al.* (1991) was based on a locally linearized part geometry. Choudhuri and De Meter (1999) considered the contact geometry between the locators and workpiece in investigating the impact of fixture locator tolerance on the geometric error of a feature.

Machine tool errors can be caused by thermal effects, cutting forces, and geometric errors in the machine tool. Various approaches have been proposed for machine tool error modeling and compensation. A volumetric error model of a three-axis jig boring machine was developed using a vector chain expression by Schultschik (1977). Ferreira and Liu (1986) developed a model to study the geometric error of a three-axis machine using a homogeneous coordinate

*Corresponding author

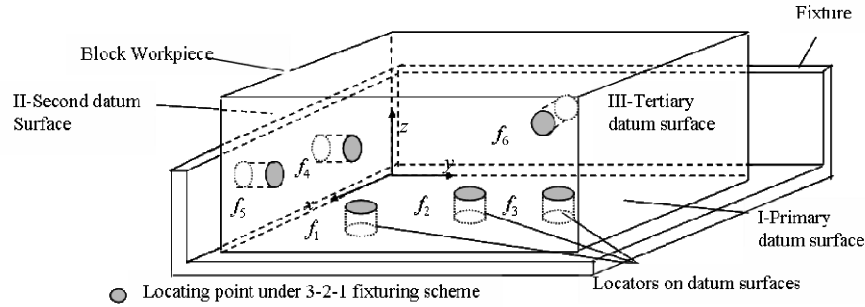


Fig. 1. Fixture locator layout.

transformation. A general methodology for modeling multi-axis machines was developed by Soons *et al.* (1992). A volumetric error model that combined geometric and thermal errors to compensate time-varying errors in real time was proposed by Chen *et al.* (1993). Other approaches, including empirical, trigonometric, and error matrix methods are summarized in Ferreira and Liu (1986).

In addition to the above literature, several studies have focused on modeling error propagation in multistage manufacturing processes (Jin and Shi, 1999; Djurdjanovic and Ni, 2001; Huang *et al.*, 2003; Zhou, Huang and Shi, 2003). A homogeneous transformation matrix was used to model the influence of errors on setup and cutting operations. Wang *et al.* (2005) studied the commonly observed phenomenon that the fixture, datum, and machine tool errors can yield the same feature deviation pattern. The concept of an Equivalent Fixture Error (EFE) was proposed to model this phenomenon. An EFE process variation model was derived by considering the impact of model formulation on root cause identification and measurement reduction in multistage machining process.

This paper uses an EFE model to investigate error cancellation in order to obtain a better understanding of the phenomenon and improved control of machining processes. Following this Introduction, in Section 2 we review the concepts behind EFE modeling. Then error cancellation is discussed in terms of EFE concepts. Section 3 analyzes the theoretical implications of the EFE model from the perspective of process monitoring and control, including root-cause diagnosis and error compensation. In Section 4, the application of the proposed diagnostic procedure is demonstrated in a machining experiment and error compensation is also illustrated in a simulation study. Conclusions are drawn in Section 5.

2. Error cancellation modeling

Wang *et al.* (2005) were the first to propose the EFE concept. The equivalent amount of locator errors that can generate the same feature deviation as that due to datum or machine tool errors was defined as being the EFE. Section 2.1 briefly introduces our notation and also reviews the EFE concept.

Section 2.2 then models error cancellation using the EFE model.

2.1. Notation and a review of the EFE concept

In a 3-2-1 locating scheme (Fig. 1), a fixture locates the workpiece through three datum surfaces, which are known as the primary, secondary, and tertiary datum surfaces, respectively. Let $\mathbf{f}_i = (f_{ix} f_{iy} f_{iz})^T$ be a point on top of locator i , $i = 1, \dots, 6$. Then the fixture error can be represented by the deviations of six locators along their axial directions:

$$\Delta \mathbf{f} = (\Delta f_{1z} \Delta f_{2z} \Delta f_{3z} \Delta f_{4y} \Delta f_{5y} \Delta f_{6x})^T. \quad (1)$$

Each surface \mathbf{X}_j is represented by its surface orientation \mathbf{v}_j and position \mathbf{p}_j (Huang *et al.*, 2003), $j = 1, 2 \dots M$, where M is the number of part surfaces. Deviations in \mathbf{X}_j are composed of deviations in \mathbf{v}_j and \mathbf{p}_j , i.e., $\mathbf{x}_j = (\Delta \mathbf{v}_j^T \Delta \mathbf{p}_j^T)^T = (\Delta v_{jx} \Delta v_{jy} \Delta v_{jz} \Delta p_{jx} \Delta p_{jy} \Delta p_{jz})^T$. The datum error is expressed as the deviations in the three datum surfaces, $\mathbf{x}_{II} \sim \mathbf{x}_{III}$.

Machine tool error is modeled as the deviation in the cutting tool path (Huang and Shi, 2003), and includes the displacement error $(x_m y_m z_m)$ and rotational error pitch α_m , roll β_m , and yaw γ_m . Using the same notation, we represent machine tool error by $\delta \mathbf{q}_m = (x_m y_m z_m \alpha_m \beta_m \gamma_m)^T$, which is invariant for all machined surfaces in an operation.

For a milling example, Fig. 2 shows the concept that the machine tool, datum, and fixture errors could generate the same error pattern. A mathematical derivation of the EFE concept is given in Appendix A.

Following Equation (1), we use $\Delta \mathbf{d} = (\Delta d_{1z} \Delta d_{2z} \Delta d_{3z} \Delta d_{4y} \Delta d_{5y} \Delta d_{6x})^T$ and $\Delta \mathbf{m} = (\Delta m_{1z} \Delta m_{2z} \Delta m_{3z} \Delta m_{4y} \Delta m_{5y} \Delta m_{6x})^T$ to represent the EFEs caused by datum and machine tool errors, respectively. Using the EFE concept allows us to transform the error sources in the machining process into fixture deviations, i.e., $\Delta \mathbf{f}$, $\Delta \mathbf{d}$, and $\Delta \mathbf{m}$. The relationship between the EFE and feature deviation can then be derived as (see more details in Appendix B)

$$\mathbf{x} = (\Gamma_u | \Gamma_u | \Gamma_u)(\Delta \mathbf{d}^T | \Delta \mathbf{f}^T | \Delta \mathbf{m}^T)^T + \varepsilon, \quad (2)$$

where \mathbf{x} is the feature deviation vector (e.g., it can be $[\mathbf{x}_1^T \mathbf{x}_2^T \dots \mathbf{x}_M^T]^T$). $\Gamma_u = [\Gamma_1^T \Gamma_2^T \dots \Gamma_M^T]^T$ is the mapping

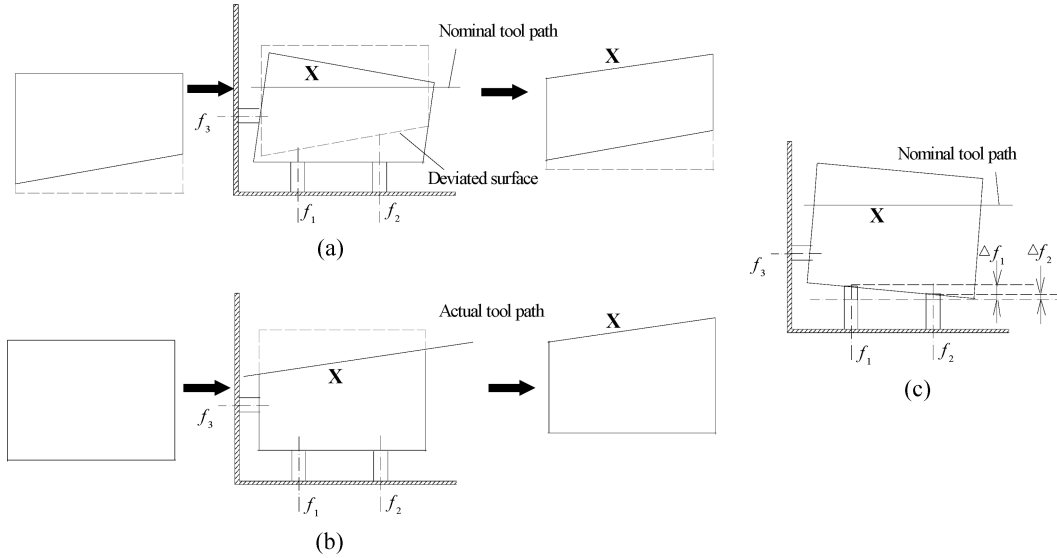


Fig. 2. The EFE concept: (a) a machining process with a datum error; (b) a machining process with a machine tool error; and (c) a machining process with a fixture error.

matrix that relates the EFE to the feature deviation. Matrix Γ_j , $j = 1, 2, \dots, M$, is the block matrix that corresponds to machined surface j . The results in Appendix B show that the Γ_j for each type of error is the same and thus the three block matrices in Equation (2) are identical. This is consistent with the phenomenon that the three error types can generate the same feature deviation.

2.2. Modeling of error cancellation

The EFE concept can be used to model error cancellation and the impact of errors on feature deviations. If we group the errors in Equation (2), we have that:

$$\mathbf{x} = \Gamma_u(\Delta\mathbf{d} + \Delta\mathbf{f} + \Delta\mathbf{m}) + \varepsilon. \quad (3)$$

Therefore, the cancellation effect of the three error types can be modeled as a linear combination of the mean shift in the EFEs and fixture error. Their impact on feature deviations can be described by using the mapping matrix Γ_u in Equation (3). For the special case where the three error types completely cancel one another, i.e., $E(\Delta\mathbf{d} + \Delta\mathbf{f} + \Delta\mathbf{m})$ is statistically insignificant, the mean of the process output is within control, where $E(\cdot)$ represents the expectation of the random variables in the parentheses. It should be noted that the variances caused by the three error types cannot be cancelled.

In this paper, $\Delta\mathbf{d}$, $\Delta\mathbf{f}$, and $\Delta\mathbf{m}$ are assumed to be independent random vectors that follow a multivariate normal distribution. ε is a random vector that follows a normal distribution $N(0, \sigma_\varepsilon^2 \mathbf{I})$. ε can be considered as the aggregated effect due to measurement noise and inherent unmodeled terms in the machining process.

The modeling approach presented in the Appendices can be applied to cases in which the datum surfaces are all

planes. When the surface is not planar, we should use the tangential plane to the surface at each locator point as the datum surface. Figure 3 shows the setup of a 2-D part with nonplanar datum surfaces. The datum surfaces are tangential planes \mathbf{T}_1 , \mathbf{T}_2 , and \mathbf{T}_3 . The corresponding normal vectors are \mathbf{n}_1 , \mathbf{n}_2 , and \mathbf{n}_3 , respectively. If the implicit form surface equation is represented by $f_j(x_j, y_j, z_j) = 0$, \mathbf{n}_j and \mathbf{p}_j are determined by:

$$\mathbf{n}_j = \left(\frac{\partial f_j}{\partial x_j}, \frac{\partial f_j}{\partial y_j}, \frac{\partial f_j}{\partial z_j} \right)^T, \quad f_j(p_{jx}, p_{jy}, p_{jz}) = 0, \quad j = \text{I, II}, \dots, \text{VI}. \quad (4)$$

Then we substitute Equation (4) into the following to compute the EFE ($\Delta\mathbf{d}$ and $\Delta\mathbf{m}$).

$$\begin{aligned} \Delta d_{iz} (\text{or } \Delta m_{iz}) &= -[n_{jx}(f_{ix} - p_{jx}) + n_{jy}(f_{iy} - p_{jy})]/n_{jz} \\ &\quad + p_{jz} - f_{iz}, \quad i = 1, 2, 3, \quad j = \text{I}, \\ \Delta d_{iy} (\text{or } \Delta m_{iy}) &= -[n_{jx}(f_{ix} - p_{jx}) + n_{jz}(f_{iz} - p_{jz})]/n_{jy} \\ &\quad + p_{jy} - f_{iy}, \quad i = 4, 5, \quad j = \text{II}, \\ \Delta d_{ix} (\text{or } \Delta m_{ix}) &= -[n_{jy}(f_{iy} - p_{jy}) + n_{jz}(f_{iz} - p_{jz})]/n_{jx} \\ &\quad + p_{jx} - f_{ix}, \quad i = 6, \quad j = \text{III}, \end{aligned} \quad (5)$$

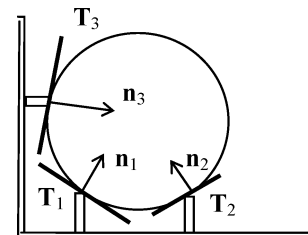


Fig. 3. Nonplanar datum surfaces.

where $(\Delta v_{jx} \Delta v_{jy} \Delta v_{jz} \Delta p_{jx} \Delta p_{jy} \Delta p_{jz})$ are the deviated datum surfaces, and $j = \text{I, II, III}$ represent three datum surfaces. Equation (5) is determined by the distance between the two points at which the locators intersect the nominal datum $\mathbf{X}_j^0 = (v_{jx}^0 v_{jy}^0 v_{jz}^0 p_{jx}^0 p_{jy}^0 p_{jz}^0)^T$ and the deviated datum surfaces $\mathbf{X}_j = (v_{jx} v_{jy} v_{jz} p_{jx} p_{jy} p_{jz})^T$.

3. Theoretical implications

The modeling of error cancellation and errors generating the same feature deviation has many implications for machining process control. Wang *et al.* (2005) found that EFE modeling could potentially lead to a reduction in the number of measurements in multistage machining processes. In this paper, we further discuss the implications on three issues: diagnosability analysis, root-cause identification, and error compensation.

3.1. Diagnosability analysis

This paper studies the diagnosability of a process that is governed by a general linear fault model that relates the errors to the feature deviation \mathbf{x} using:

$$\mathbf{x} = \Gamma(\mathbf{x}_D^T \Delta \mathbf{f}^T \delta \mathbf{q}_m^T)^T + \varepsilon, \quad (6)$$

where matrix Γ is determined by the part design. Its relationship with Γ_u will be discussed in Proposition 1. $\mathbf{x}_D = (\mathbf{x}_I^T \mathbf{x}_{II}^T \mathbf{x}_{III}^T)^T$ is the error vector of the three datum surfaces of the raw workpiece.

If the process is diagnosable, then a Least Squares Estimation (LSE) can be performed, i.e.,

$$(\mathbf{x}_D^T \Delta \mathbf{f}^T \delta \mathbf{q}_m^T)^T = (\Gamma^T \Gamma)^{-1} \Gamma^T \mathbf{x}. \quad (7)$$

The diagnosability depends on the rank of Γ (Zhou, Ding, Chen and Shi, 2003). We can see that Equation (7) requires $\Gamma^T \Gamma$ to be full rank, or equivalently, all the columns in Γ to be independent. Proposition 1 addresses the structure of Γ for a machining process.

Proposition 1. *In Equation (6) the block matrices in matrix Γ that correspond to the three error type are dependent and matrix $\Gamma^T \Gamma$ is always not full rank, i.e., the fixture, datum, and machine tool errors cannot be distinguished by solely measuring the part features.*

Proof. If we use the transformation matrices \mathbf{K}_1 (Equation (A.1)) and \mathbf{K}_2 (Equation (A.2)) to map the datum error \mathbf{x}_D to $\Delta \mathbf{d}$ and the machine tool error $\delta \mathbf{q}_m$ to $\Delta \mathbf{m}$, respectively, Equation (2) becomes:

$$\mathbf{x} = [\Gamma_u \mathbf{K}_1 \mid \Gamma_u \mid \Gamma_u \mathbf{K}_2](\mathbf{x}_D^T \mid \Delta \mathbf{f}^T \mid \delta \mathbf{q}_m^T)^T + \varepsilon. \quad (8)$$

Comparing Equation (8) with Equation (6), we get that $\Gamma = [\Gamma_u \mathbf{K}_1 \Gamma_u \Gamma_u \mathbf{K}_2]$. However, the columns that correspond to the fixture and machine tool errors in matrix Γ are linearly dependent because the columns of $\Gamma_u \mathbf{K}_1$ and $\Gamma_u \mathbf{K}_2$ are linear combination of the columns of Γ_u . Therefore, the rank of Γ is equal to the rank of Γ_u . This also implies that the system is not diagnosable. ■

An implication of this proposition is that a LSE cannot be obtained. However, the fault model of Equation (3) with the errors grouped eliminates the linearly dependent columns in matrix Γ . This fact leads to sequential root-cause identification which is discussed in Section 3.2.

3.2. Sequential root cause identification

Using Equation (3), the grouped errors \mathbf{u} can be estimated as:

$$\hat{\mathbf{u}}^{(n)} = \Delta \hat{\mathbf{d}}^{(n)} + \Delta \hat{\mathbf{f}}^{(n)} + \Delta \hat{\mathbf{m}}^{(n)} = (\Gamma_u^T \Gamma_u)^{-1} \Gamma_u^T \mathbf{x}^{(n)}, \quad n = 1, 2, \dots, N, \quad (9)$$

where $\hat{\mathbf{u}}^{(n)}$ is the LSE of \mathbf{u} for the n th replicate of the measurement. Each row of Γ_u corresponds to an output feature whereas each column of Γ_u corresponds to a component in the error vectors. Hence, the number of rows of Γ_u must be larger than the number of columns to ensure that sufficient features are measured for LSE.

Denote $\Delta f_i^{(n)}$, $\Delta d_i^{(n)}$, and $\Delta m_i^{(n)}$ as the i th component of the vectors $\Delta \mathbf{f}^{(n)}$, $\Delta \mathbf{d}^{(n)}$, and $\Delta \mathbf{m}^{(n)}$, respectively. We can develop a strategy for root cause identification that involves the following steps:

1. Necessary error information is collected first to identify the existence of error sources using Equation (9). The process error information can be analyzed by conducting a hypothesis test on $\{\hat{\mathbf{u}}^{(n)}\}_{n=1}^N$. Since the estimated \mathbf{u} is a mixture of noise and errors, a proper test statistic should be developed to detect the faults due to process noise. Hypothesis tests on the mean and variance can then be used to find out if the faults are mean shift or large variance in nature
2. Additional measurement on the locator deviation ($\Delta f_i^{(n)}$) and datum error ($\Delta d_i^{(n)}$) of the raw workpiece is conducted (due to Proposition 1) to distinguish between different types of errors. The mean shift of the errors can be estimated using the sample mean of $\Delta d_i^{(n)}$, $\Delta f_i^{(n)}$, and $\Delta m_i^{(n)} = u_i^{(n)} - \Delta d_i^{(n)} - \Delta f_i^{(n)}$. The variance can then be estimated by the sample variance for $\Delta d_i^{(n)}$, $\Delta f_i^{(n)}$, and $\Delta m_i^{(n)}$.

This approach can effectively identify the machine tool errors. The detailed procedures will be given in Section 4.

3.3. Error compensation

We can use the error cancellation effect to compensate for process errors. With the development of an adjustable fixture whose locator length is changeable, it is feasible to compensate errors by simply changing the length of the locators. We use the index i to represent the i th adjustment period. During period i , N part feature deviations $\{\mathbf{x}^{(n)}\}_{n=1}^N$ are measured to determine the amount of locator adjustment.

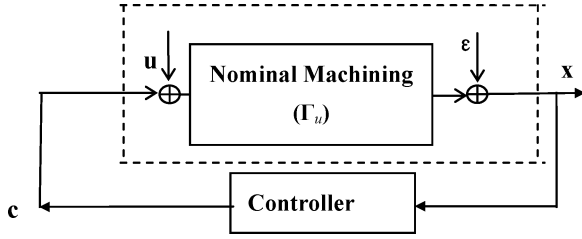


Fig. 4. Error compensation for a disturbed process.

Such a compensation is only implemented at the beginning of a period. Denote \mathbf{c}^i as the accumulated value of the locator length adjustments after the i th period but before the beginning of period $i + 1$. The compensation procedure is illustrated in Fig. 4. One can see that a nominal machining process is disturbed by errors $\Delta \mathbf{d}$, $\Delta \mathbf{f}$, and $\Delta \mathbf{m}$, and the observation noise ε . Error sources, noise, and the machining process constitute a disturbed process, as marked in the dashed line block. Using the feature deviation \mathbf{x}^i for the i th period as the input (\mathbf{x}^i can be estimated as the average of N measured parts in the period i , i.e., $\hat{\mathbf{x}}^i = 1/N \sum_{n=1}^N \mathbf{x}^{i(n)}$), a controller is introduced to generate signal \mathbf{c}^i that manipulates adjustable fixture locators so as to counteract the errors for the $(i + 1)$ th machining period. The amount of compensation at period $i + 1$ should be $\mathbf{c}^i - \mathbf{c}^{i-1}$. The error compensation model can then be written as:

$$\mathbf{x}^{i+1} = \mathbf{S}^{i+1} + \Gamma_u \mathbf{c}^i \quad \text{and} \quad \mathbf{S}^{i+1} = \Gamma_u \mathbf{u}^{i+1} + \varepsilon^{i+1}, \quad (10)$$

where \mathbf{S}^{i+1} is the output of the disturbed process for time $i + 1$. This term represents the feature deviation measured without any compensation being made.

In this paper, we focus on static errors because they account for the majority of machining errors (Zhou, Huang, and Shi, 2003). A negative value for predicted EFEs means that they can be used to adjust the locators. Thus, we derive an integral control that can minimize the Mean Square Error (MSE) of the feature deviation, i.e.,

$$\mathbf{c}^i = -(\Gamma_u^T \Gamma_u)^{-1} \Gamma_u^T \sum_{t=1}^i \mathbf{x}^t = -\sum_{t=1}^i (\Delta \hat{\mathbf{d}}^t + \Delta \hat{\mathbf{f}}^t + \Delta \hat{\mathbf{m}}^t). \quad (11)$$

Equation (11) shows that the accumulated amount of compensation for the next period is equal to the sum of the LSE of the EFEs of the current and all the previous time periods of the machining process. The accumulated compensation \mathbf{c}^i can be used to evaluate the controller performance in stability and robustness analyses. The amount of compensation for the $(i + 1)$ th period is $\mathbf{c}^i - \mathbf{c}^{i-1}$:

$$\mathbf{c}^i - \mathbf{c}^{i-1} = -(\Gamma_u^T \Gamma_u)^{-1} \Gamma_u^T \mathbf{x}^i. \quad (12)$$

The compensation accuracy can be estimated by $\Gamma_u[\mathbf{u} - (\Gamma_u^T \Gamma_u)^{-1} \Gamma_u^T \mathbf{x}^i] = \mathbf{x}^i - \Gamma_u(\Gamma_u^T \Gamma_u)^{-1} \Gamma_u^T \mathbf{x}^i$, i.e., the difference between \mathbf{x}^i and its LSE. Denote the range space of Γ_u as $R(\Gamma_u)$ and the null space of Γ_u^T as $N(\Gamma_u^T)$. Spaces $R(\Gamma_u)$ and $N(\Gamma_u^T)$ are orthogonal and constitute the whole vector

space $\mathbf{R}^{q \times 1}$, where q is the number of rows in \mathbf{x}^i (or Γ_u). By the LSE property we know that the estimation error vector $\mathbf{x}^i - \Gamma_u(\Gamma_u^T \Gamma_u)^{-1} \Gamma_u^T \mathbf{x}^i$ is orthogonal to $R(\Gamma_u)$. Therefore, the compensation accuracy of Equation (12) can be estimated by the projection of the observation (feature deviation) vector \mathbf{x}^i onto $N(\Gamma_u^T)$. This conclusion also shows the components of the observation that can be compensated. The projection of the observation vector \mathbf{x}^i onto space $R(\Gamma_u)$ can be fully compensated by using Equation (12) whereas the projection onto $N(\Gamma_u^T)$ cannot be compensated.

In practice, the accuracy that the adjustable locator can achieve must be considered. Suppose that the standard deviation of a locator's movement is σ_f . We can set the stopping region for applying error compensation with a 99.73% confidence level as:

$$-3\sigma_f \leq \mathbf{c}^i - \mathbf{c}^{i-1} \leq 3\sigma_f. \quad (13)$$

4. Case studies

The discussion in Section 3 has highlighted the application of the EFE concept to sequential root-cause identification and error compensation. The diagnostic algorithm for these effects is proposed in this section and demonstrated by its application to a machining experiment. EFE compensation for process control is illustrated by a simulation study.

4.1. Root-cause identification

There are several diagnostic approaches (Ceglarek and Shi, 1996; Apley and Shi, 1998; Rong *et al.*, 2001) that have achieved considerable success in fixture fault detection. The approach proposed by Apley and Shi (1998) can effectively identify multiple fixture faults. By extending this approach, we use it for sequential root-cause identification:

Step 1. Conduct measurements on the features and datum surfaces of the raw workpiece so as to estimate the error sources $\hat{\mathbf{u}}^{(n)}$ for each replicate using Equation (9). The grouped error can be estimated by the average of $\hat{\mathbf{u}}^{(n)}$ over N measured workpieces, i.e., $\hat{\mathbf{u}} = (1/N) \sum_{n=1}^N \hat{\mathbf{u}}^{(n)}$, $n = 1, 2, \dots, N$. As mentioned in Section 3.2, the fault vector \mathbf{u} contains both error sources and process noise.

Step 2. To detect those faults due to process noise, we can use the F -test statistic introduced by Apley and Shi (1998):

$$F_i = \frac{\hat{S}_i^2}{[(\Gamma_u^T \Gamma_u)^{-1}]_{i,i} \hat{S}_\varepsilon^2}, \quad i = 1, 2, \dots, 6, \quad (14)$$

where $\hat{S}_i^2 = (1/N) \sum_{n=1}^N [\hat{u}_i^{(n)}]^2$, and $\hat{u}_i^{(n)}$ represents the i th component of vector $\hat{\mathbf{u}}^{(n)}$. $(\Gamma_u^T \Gamma_u)^{-1}_{i,i}$ is the i th diagonal entry of matrix $(\Gamma_u^T \Gamma_u)^{-1}$. The estimator

for the variance of the noise is:

$$\hat{S}_\varepsilon^2 = \frac{1}{N(q-6)} \sum_{n=1}^N \hat{\varepsilon}(n)^T \hat{\varepsilon}(n),$$

and $\hat{\varepsilon}^{(n)} = \mathbf{x}^{(n)} - \Gamma_u \hat{\mathbf{u}}^{(n)}$ is for the noise term. When $F_i > F_{1-\alpha}(N, N(q-6))$, we conclude that the i th fault occurs with a confidence level of $100(1-\alpha)\%$. By investigating $\{\hat{u}_i^{(n)}\}_{n=1}^N$ for mean u_i ($H_0: u_i = 0$ vs. $H_1: u_i \neq 0$), and variance σ_{ui}^2 ($H_0: \sigma_{ui}^2 \leq \sigma_0^2$ vs. $H_1: \sigma_{ui}^2 > \sigma_0^2$), one can determine whether the error pattern of the faults is mean shift or variance type. σ_0^2 is a small value. In the case study, we choose $\sigma_0^2 = 0.1 \text{ mm}^2$. By the normality assumption of EFEs ($\Delta \mathbf{d}$, $\Delta \mathbf{f}$, and $\Delta \mathbf{m}$), we can use the T test statistic.

$$T = u_i / \sqrt{\frac{1}{N(N-1)} \sum_{n=1}^N (u_i^{(n)} - u_i)^2},$$

and compare it with $t_{1-\alpha/2}(n-1)$ to test the mean shift. $\chi^2 = \sum_{n=1}^N (u_i^{(n)} - u_i)^2 / \sigma_0^2$ is used and compared with $\chi_{1-\alpha}^2(n-1)$ to test the variance. α is the significance level. If $F_i < F_{1-\alpha}(N, N(q-6))$, either no faults occur at the i th locator, or the faults cannot be distinguished from process noise.

Step 3. Use additional measurements to distinguish errors whenever faults are identified. The locator deviation $\{\Delta f_i^{(n)}\}_{n=1}^N$ and the datum surfaces $\{\mathbf{X}_j^{(n)}\}_{n=1}^N$ are measured. The EFE $\{\Delta d_i^{(n)}\}_{n=1}^N$ caused by the datum errors can be calculated using Equation (A.1). If the errors turn out to be a mean shift ($u_i \neq 0$ for a certain i), the machine tool error in terms of the EFE is $\Delta \hat{m}_i = \hat{u}_i - \Delta d_i - \Delta f_i$, where Δd_i and Δf_i are the average EFE over all N parts. The machine tool error $\delta \mathbf{q}_m$ is then determined by the inverse of Equation (A2):

$$\delta \mathbf{q}_m = \mathbf{K}_2^{-1} \Delta \mathbf{m}. \tag{15}$$

The variance of grouped error (σ_{ui}^2) can then be decomposed as:

$$\sigma_{ui}^2 = \sigma_{di}^2 + \sigma_{fi}^2 + \sigma_{mi}^2. \tag{16}$$

If $\sigma_{ui}^2 > \sigma_0^2$, the variances caused by the three types of errors σ_{di}^2 , σ_{fi}^2 , and σ_{mi}^2 can be estimated by the sample variance of $\{\Delta d_i^{(n)}\}_{n=1}^N$, $\{\Delta f_i^{(n)}\}_{n=1}^N$, and $\{\Delta \hat{m}_i^{(n)}\}_{n=1}^N$.

The $100(1-2\alpha)\%$ Confidence Interval (CI) of $\Delta \mathbf{m}$ is $(\Delta \hat{\mathbf{m}} \pm \mathbf{L})$, where $z_{1-\alpha}$ follows the cumulative standard normal distribution such that:

$$\int_{-\infty}^{z_{1-\alpha}} \frac{1}{\sqrt{2\pi}} e^{-u^2/2} du = 1 - \alpha, \text{ and } \mathbf{L} = \left| \left(z_{1-\alpha} \sqrt{(\Gamma_u^T \Gamma_u)^{-1}_{1,1}} \hat{\sigma}_\varepsilon \dots z_{1-\alpha} \sqrt{(\Gamma_u^T \Gamma_u)^{-1}_{6,6}} \hat{\sigma}_\varepsilon \right)^T \right|_{6 \times 1}.$$

The corresponding CI vector for $\delta \mathbf{q}_m$ is $(\mathbf{K}_2^{-1} \Delta \mathbf{m} \pm \mathbf{K}_2^{-1} \mathbf{L})$. The CI for $\Delta \mathbf{d}$ and $\Delta \mathbf{f}$ can be obtained by $(\Delta d_i \pm S_{di} t_{1-\alpha/2}(n-1) / \sqrt{n})$ and $(\Delta f_i \pm S_{fi} t_{1-\alpha/2}(n-1) / \sqrt{n})$, where S_{di} and S_{fi} are the sample variance for $\{\Delta d_i^{(n)}\}_{n=1}^N$ and $\{\Delta f_i^{(n)}\}_{n=1}^N$.

To demonstrate the model and the diagnostic procedure, we intentionally introduced datum and machine tool errors in the milling of five block workpieces. We used the same setup, raw workpiece and fixturing scheme as Wang *et al.* (2005) (Fig. 5). A xyz coordinate system fixed with a nominal fixture is also introduced to represent the plane. The top plane \mathbf{X}_1 and the side plane \mathbf{X}_2 are to be milled. Eight vertices are marked as 1–8 and their coordinates in the xyz coordinate system are measured to help to determine \mathbf{X}_1 and \mathbf{X}_2 . In this paper, the units are millimeters for length and radians for angle. For the coordinate system of Fig. 5, the surface specifications are $\mathbf{X}_1 = (0 \ 0 \ 1 \ 0 \ 0 \ 15.24)^T$, and $\mathbf{X}_2 = (0 \ 1 \ 0 \ 0 \ 96.5 \ 0)^T$. From Equation (3) and Equation (A8), we get

$$\mathbf{x}^i = \begin{pmatrix} \Gamma_1 \\ \Gamma_2 \end{pmatrix} (\Delta \mathbf{d}^i + \Delta \mathbf{f}^i + \Delta \mathbf{m}^i) + \varepsilon^i,$$

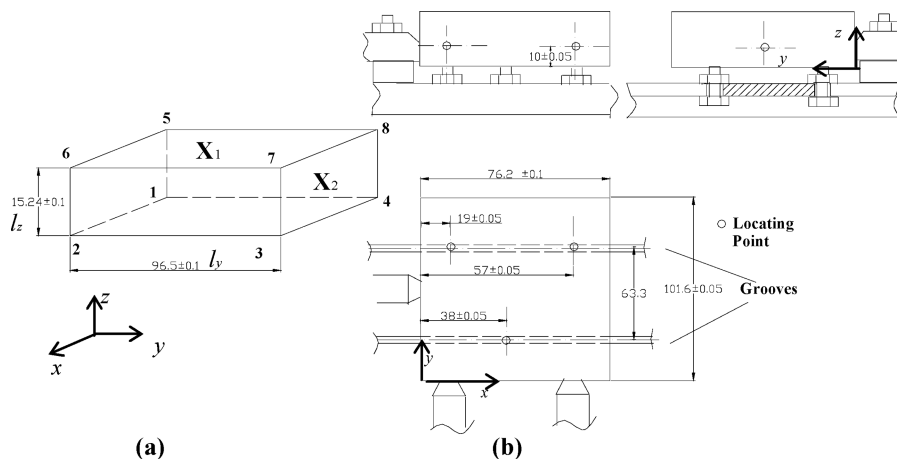


Fig. 5. Nominal part, tolerance, and fixture layout (after Wang *et al.* (2005)).

Table 1. Measured features in units of millimeters

<i>n</i>	<i>X</i> ₁					<i>X</i> ₂				
	1	2	3	4	5	1	2	3	4	5
Δv_x	-0.001	-0.001	0.001	-0.001	0.001	0.001	-0.001	0.001	0.001	0.001
Δv_y	-0.033	-0.034	-0.039	-0.034	-0.035	0.001	0.001	0.001	0.001	0.001
Δv_z	0.001	-0.001	0.001	0.001	0.001	0.032	0.034	0.032	0.036	0.035
Δp_x	0.001	-0.001	0.001	0.001	0.001	0.001	0.001	0.001	0.001	0.001
Δp_y	-0.145	-0.163	-0.119	-0.185	-0.153	0.347	0.379	0.253	0.307	0.268
Δp_z	-3.877	-2.749	-2.329	-3.509	-2.459	0.579	0.358	0.479	0.539	0.429

where

$$\Gamma_1 = \begin{pmatrix} 0 & -0.0263 & 0.0263 & 0 & 0 & 0 \\ -0.0158 & 0.0079 & 0.0079 & 0 & 0 & 0 \\ 0 & 0 & 0 & 0 & 0 & 0 \\ 0 & -0.1379 & 0.1379 & 1.3368 & -1.3368 & -1 \\ -0.0828 & 0.0414 & 0.0414 & -1.5 & 0.5 & 0 \\ -1.3033 & -0.8483 & 1.1517 & 0 & 0 & 0 \end{pmatrix},$$

$$\Gamma_2 = \begin{pmatrix} 0 & 0 & 0 & -0.0263 & 0.0263 & 0 \\ 0 & 0 & 0 & 0 & 0 & 0 \\ 0.0158 & -0.0079 & -0.0079 & 0 & 0 & 0 \\ 0 & 0.2632 & -0.2632 & -1.2026 & 1.2026 & -1 \\ 0.158 & -0.079 & -0.079 & -1.5 & 0.5 & 0 \\ 0.2212 & -1.6106 & 0.3894 & 0 & 0 & 0 \end{pmatrix}.$$

The number of rows *q* in Γ is 12. We set fixture error to be zero ($\Delta \mathbf{f} = 0$). The primary datum plane I is pre-machined to be $\mathbf{X}_I = (0 \ 0.018 \ -0.998 \ 0 \ 0.207 \ -1.486)^T$ and its corresponding EFE is $\Delta \mathbf{d} = (1.105 \ 0 \ 0 \ 0 \ 0 \ 0)^T$ mm. The machine tool error is set to be $\delta \mathbf{q}_m = (0 \ 0.175 \ -1.44 \ 0.0175 \ 0 \ 0)^T$ by adjusting the orientation and position of the tool path. Based on the measured coordinates of vertices 1–8, the obtained feature deviations are listed in Table 1.

The EFE faults identified after following Steps 1–3 are listed in Tables 2 and 3.

Take α to be 0.01. Then the threshold value $F_{0.99}(5, 5(12 - 6)) = F_{0.99}(5, 30) = 3.699$. In Table 3, we can see that

$F_1 > 3.699$, which indicates that a fault occurs at locator 1. Using the data in the first row of Table 2 to conduct *T* and χ^2 tests for mean and variance, we find that $T > t_{1-0.01/2}(5 - 1) = t_{0.995}(4) = 4.604$ and $\chi^2 < \chi^2_{1-0.01}(4) = 13.277$. Hence, we conclude that there is a significant mean shift whereas the variance is not large. If we make additional measurements, by Equation (A2), the 98% CI for the detected mean shift of the machine tool error is $\delta \mathbf{q}_m = (0.006 \ 0.167 \ -1.540 \ 0.018 \ -0.000 \ 0.000)^T \pm (0.008 \ 0.001 \ 0.000 \ 0.000 \ 0.001 \ 0.000)^T$, which is consistent with the pre-introduced errors. The EFE fault model and diagnostic algorithm is therefore experimentally validated.

4.2. Error compensation simulation

Using the same machining process as in Section 4.1, we can simulate error compensation over five adjustment periods. Five parts are sampled during each period. We set the fixture error to be $\Delta \mathbf{f} = (0.276 \ 0 \ 0 \ 0.276 \ 0 \ 0)^T$ mm. The machine tool error is set to be $\delta \mathbf{q}_m = (-0.075 \ -0.023 \ 0.329 \ -0.0023 \ 0.0075 \ 0)^T$ and its EFE is $\Delta \mathbf{m} = (0 \ 0 \ 0.286 \ 0 \ 0 \ 0)^T$ mm. We assume that the measurement noise follows $N(0, (0.002 \text{ mm})^2)$ for the displacement and $N(0, (0.001 \text{ rad})^2)$ for the orientation. The compensation values can be calculated using Equations (11) and (12). In this case study, the accuracy of the locator movement is assumed to be $\sigma_f = 0.01$ mm and the criterion for stopping the compensation is $-0.03 \leq \mathbf{c}^i - \mathbf{c}^{i-1} \leq 0.03$ mm (Equation (13)). Figure 6 shows the compensation ($\mathbf{c}^i - \mathbf{c}^{i-1}$) for locators f_1 – f_4 . The values of adjustment periods 2–5 are given by the solid line in the figure. The dash-dot line represents the

Table 2. Estimation of \mathbf{u} for five replicates in units of millimeters

$\hat{\mathbf{u}}^{(1)}$	$\hat{\mathbf{u}}^{(2)}$	$\hat{\mathbf{u}}^{(3)}$	$\hat{\mathbf{u}}^{(4)}$	$\hat{\mathbf{u}}^{(5)}$	$\hat{\mathbf{u}}$	<i>T</i>	χ^2
2.937	2.133	1.775	2.697	1.902	2.289	10.119	10.247
0.050	0.090	-0.064	0.057	0.002	0.027	—	—
0.002	0.090	-0.0562	0.057	0.020	0.023	—	—
0.055	-0.031	0.003	0.039	0.015	0.016	—	—
0.047	-0.031	0.004	0.039	0.018	0.015	—	—
0.004	0.000	-0.001	0.000	-0.001	0.001	—	—

Table 3. Additional measurement results in units of millimeters

Locators	\hat{u}	F_i	Δf	Δd	Δm
1	2.289	19.525	0	1.105	1.184
2	0.027	0.051	0	0	0.027
3	0.023	0.005	0	0	0.023
4	0.016	0.613	0	0	0.016
5	0.015	0.073	0	0	0.015
6	0.001	0.002	0	0	0.003

value of $\pm 3\sigma_f$. The adjustment for locators f_5 and f_6 are all zero and not shown in the figure. One can see that the effect of compensation in the second period is dominant. The compensation for the subsequent periods is relatively small because no significant error sources are introduced in these periods.

The effect of error compensation can be illustrated with the quality improvement of two features, the plane distance along the z axis (l_z) and the y axis (l_y) as shown in Fig. 5. l_z can be estimated by the mean and standard deviation of the lengths of edges l_{15} , l_{26} , l_{37} , and l_{48} and l_y can be estimated by l_{14} , l_{23} , l_{67} , and l_{58} for each machining period, where l_{mn} is the distance between the vertices m and n and is estimated by the edge length of five parts in each period. The milling of planes X_1 and X_2 impacts on the plane distance along the z and y axes. The nominal part should have the same edge lengths along the z and y directions (15.24 and 96.5 mm, see the dashed line in Fig. 7), respectively. However, in the first adjustment period ($i = 1$) without error compensation, the standard error of the edge lengths are beyond the specified tolerance. In periods 2–5 when the compensation algorithm is applied the deviations of l_z and l_y are significantly reduced.

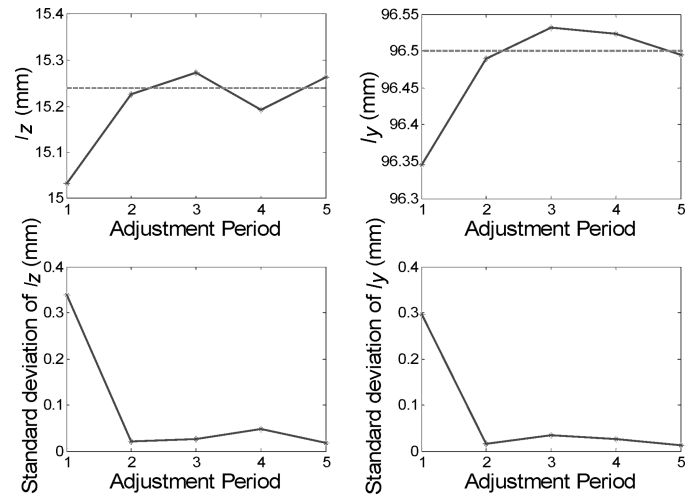


Fig. 7. Mean and standard deviation of the two features.

5. Conclusions

This paper has investigated error cancellation among datum, fixture, and machine tool errors as a method to improve quality control in machining processes. Based on the EFE concept error cancellation was modeled as a linear combination of EFEs. A process fault model was then derived in terms of grouped EFEs to allow us to conduct a fault diagnosis and error compensation of a machining process. The EFE methodology helped to reveal the structure of the matrix of the fault model. We mathematically proved that a machining process with datum, fixture, and machine tool errors cannot be diagnosed by simply measuring the part features. To solve this problem, we developed the procedure of sequential root-cause identification. First, datum error and machine tool error are grouped with the fixture

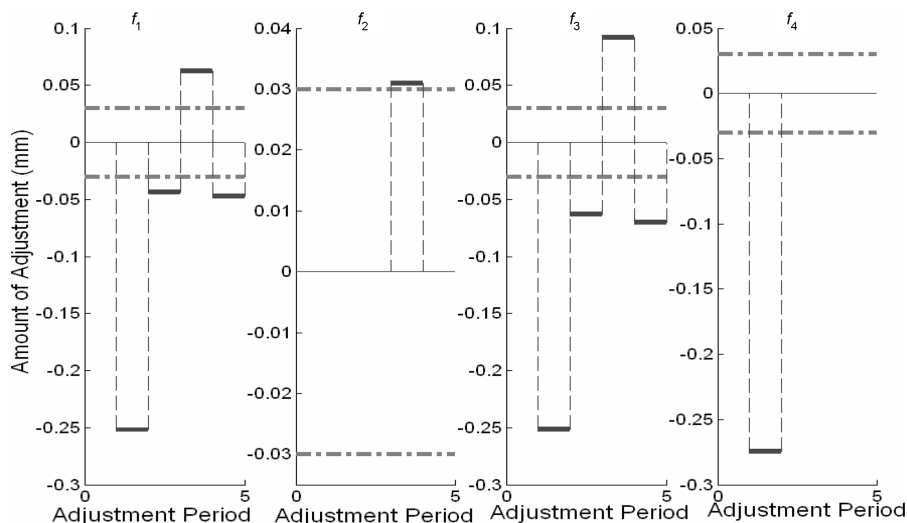


Fig. 6. Error compensation for each locator.

error and the existence and locations of EFEs is detected. Additional measurements on the process variable (locator deviation) only need to be implemented if faults are detected. This procedure can detect the mean shift and variance of process faults from the process noise. A case study of a milling process of block parts has shown that the proposed approach can effectively identify the error sources. An error cancellation study has also suggested that the machine tool and datum errors can be compensated by adjusting the length of the fixture locators. An integral control algorithm for the compensation of static errors has been presented. The procedure was demonstrated by means of a simulation study.

A future area of study involves applying the EFE concept to processes with dynamic disturbances so as to determine the disturbance model and find out the optimal control rule to minimize the MSE.

References

- Apley, D.W. and Shi, J. (1998) Diagnosis of multiple fixture faults in panel assembly. *Transactions of the ASME, Journal of Manufacturing Science and Engineering*, **120**, 793–801.
- Asada, H. and By, A.B. (1985) Kinematic analysis of workpart fixturing for flexible assembly with automatically reconfigurable fixtures. *IEEE Transactions on Robotics and Automation*, **1**, 86–94.
- Ball, R.S. (1900) *A Treatise on the Theory of Screws*, Cambridge University Press, Cambridge, UK.
- Cai, W., Hu, S. and Yuan, J. (1997) Variational method of robust fixture configuration design for 3-d workpiece. *Transactions of the ASME, Journal of Manufacturing Science and Engineering*, **119**, 593–602.
- Ceglarek, D. and Shi, J. (1996) Fixture failure diagnosis for auto body assembly using pattern recognition. *Transactions of the ASME, Journal of Engineering for Industry*, **118**, 55–65.
- Chen, J.S., Yuan, J.X., Ni, J. and Wu, S.M. (1993) Real-time compensation for time-variant volumetric errors on a machining center. *Transactions of the ASME, Journal of Engineering for Industry*, **115**, 72–79.
- Choudhuri, S.A. and De Meter, E.C. (1999) Tolerance analysis of machining fixture locators. *Transactions of the ASME, Journal of Manufacturing Science and Engineering*, **121**, 273–281.
- Djurdjanovic, D. and Ni, J. (2001) Linear state space modeling of dimensional errors. *Transactions of NAMRI/SME*, **29**, 541–548.
- Ferreira, P.M. and Liu, C.R. (1986) A contribution to the analysis and compensation of the geometric error of a machining center. *Annals of the CIRP*, **35**, 259–262.
- Huang, Q. and Shi, J. (2003) Simultaneous tolerance synthesis through variation propagation modeling of multistage manufacturing processes. *NAMRI/SME Transactions*, **31**, 515–522.
- Huang, Q., Shi, J. and Yuan, J. (2003) Part dimensional error and its propagation modeling in multi-operational machining processes. *Transactions of the ASME, Journal of Manufacturing Science and Engineering*, **125**, 255–262.
- Jin, J. and Shi, J. (1999) State space modeling of sheet metal assembly for dimensional control. *Transactions of the ASME, Journal of Manufacturing Science and Engineering*, **121**, 756–762.
- Marin, R. and Ferreira, P. (2003) Analysis of influence of fixture locator errors on the compliance of the work part features to geometric tolerance specification. *Transactions of the ASME, Journal of Manufacturing Science and Engineering*, **125**, 609–616.
- Ohwovoriole, E.N. and Roth, B. (1981) An extension of screw theory. *Transactions of the ASME, Journal of Mechanical Design*, **103**, 725–734.
- Rong, Q., Shi, J. and Ceglarek, D. (2001) Adjusted least square approach for diagnosis of ill-conditioned compliant assemblies. *Transactions of the ASME, Journal of Manufacturing Science and Engineering*, **123**, 453–461.
- Schultschik, R. (1977) The components of the volumetric accuracy. *Annals of the CIRP*, **26**, 223–228.
- Shawki, G.S.A. and Abdel-Aal, M.M. (1965) Effect of fixture rigidity of and wear on dimensional accuracy. *International Journal of Machine Tool Design and Research*, **5**, 183–202.
- Soons, J.A., Theuvs, F.C., and Schellekens, P.H. (1992) Modeling the errors of multi-axis machines: a general methodology. *Precision Engineering*, **14**, 5–19.
- Wang, H., Huang, Q. and Katz, R. (2005) Multi-operational machining processes modeling for sequential root cause identification and measurement reduction. *Transactions of the ASME, Journal of Manufacturing Science and Engineering*, **127**, 512–521.
- Weill, R., Darel, I. and Laloum, M. (1991) The influence of fixture positioning errors on the geometric accuracy of mechanical parts, in *Proceedings of the CIRP Conference on PE & ME*, pp. 215–225.
- Zhou, S., Huang, Q. and Shi, J. (2003) State space modeling of dimensional variation propagation in multistage machining process using differential motion vectors. *IEEE Transaction on Robotics and Automation*, **19**, 296–309.
- Zhou, S., Ding, Y., Chen, Y. and Shi, J. (2003) Diagnosability study of multistage manufacturing processes based on linear mixed-effects models. *Technometrics*, **45**, 312–325.

Appendices

Appendix A: Derivation of the EFE

Assume that all of the three datum surfaces are planar. By linearizing Equation (5), we can derive the EFE ($\Delta d_{ix} \Delta d_{iy} \Delta d_{iz}$) caused by the datum error as:

$$\Delta d_{iz} = -f_{ix} \Delta v_{Ix} - f_{iy} \Delta v_{Iy} - \Delta p_{Iz}, \quad i = 1, 2, 3,$$

$$\Delta d_{iy} = -f_{ix} \Delta v_{IIx} - f_{iz} \Delta v_{IIz} - \Delta p_{IIy}, \quad i = 4, 5,$$

$$\text{or } \Delta \mathbf{d} = \mathbf{K}_1 \begin{pmatrix} \mathbf{x}_I \\ \mathbf{x}_{II} \\ \mathbf{x}_{III} \end{pmatrix}.$$

$$\Delta d_{ix} = -f_{iy} \Delta v_{IIIy} - f_{iz} \Delta v_{IIIz} - \Delta p_{IIIx}, \quad i = 6. \quad (\text{A1})$$

The mapping matrix that relates the datum error to $\Delta \mathbf{d}$ is:

$$\mathbf{K}_1 = \begin{pmatrix} \mathbf{G}_1 & 0 & 0 \\ 0 & \mathbf{G}_2 & 0 \\ 0 & 0 & \mathbf{G}_3 \end{pmatrix},$$

where

$$\mathbf{G}_1 = - \begin{pmatrix} f_{1x} & f_{1y} & 0 & 0 & 0 & 1 \\ f_{2x} & f_{2x} & 0 & 0 & 0 & 1 \\ f_{3x} & f_{3x} & 0 & 0 & 0 & 1 \end{pmatrix},$$

$$\mathbf{G}_2 = - \begin{pmatrix} f_{4x} & 0 & f_{4z} & 0 & 1 & 0 \\ f_{5x} & 0 & f_{5z} & 0 & 1 & 0 \end{pmatrix},$$

$$\text{and } \mathbf{G}_3 = -(0 \quad f_{6y} \quad f_{6z} \quad 1 \quad 0 \quad 0).$$

When deriving $\Delta \mathbf{m}$, we use the relationship between \mathbf{X}_j and the machine tool error $\delta \mathbf{q}_m$. Linearization of Equation (5) then yields:

$$\Delta \mathbf{m} = \mathbf{K}_2 \delta \mathbf{q}_m, \quad (\text{A2})$$

where

$$\mathbf{K}_2 = \begin{pmatrix} 0 & 0 & -1 & -f_{1y} & f_{1x} & 0 \\ 0 & 0 & -1 & -f_{2y} & f_{2x} & 0 \\ 0 & 0 & -1 & -f_{3y} & f_{3x} & 0 \\ 0 & -1 & 0 & f_{4z} & 0 & -f_{4x} \\ 0 & -1 & 0 & f_{5z} & 0 & -f_{5x} \\ -1 & 0 & 0 & 0 & -f_{6z} & f_{6y} \end{pmatrix}.$$

Note that if the datum surfaces are not planes then the datum surfaces \mathbf{X}_j become tangential planes to each locating point and there are then six datum surfaces.

Appendix B: Derivation of Γ_j

Huang and Shi (2003) have modeled the setup and cutting operation using a homogeneous transformation matrix. Feature deviation can then be expressed (Wang *et al.*, 2005):

$$\mathbf{x}_j = (\mathbf{A}_{jd} \mid \mathbf{A}_{jf} \mid \mathbf{A}_{jm}) \delta \mathbf{q} + \boldsymbol{\varepsilon}_j, \quad (\text{A3})$$

where

$$\mathbf{A}_{jd}(k) = \mathbf{A}_{jf}(k) = -\mathbf{A}_{jd}(k) = \begin{pmatrix} 0 & 0 & 0 & 0 & -2v_{jz}^0 & 2v_{jy}^0 \\ 0 & 0 & 0 & 2v_{jz}^0 & 0 & -2v_{jx}^0 \\ 0 & 0 & 0 & -2v_{jy}^0 & 2v_{jx}^0 & 0 \\ -1 & 0 & 0 & 0 & -2p_{jz}^0 & 2p_{jy}^0 \\ 0 & -1 & 0 & 2p_{jz}^0 & 0 & -2p_{jx}^0 \\ 0 & 0 & -1 & -2p_{jy}^0 & 2p_{jx}^0 & 0 \end{pmatrix}, \text{ and } \text{rank}(\mathbf{A}_{jd}) \leq 5.$$

$\delta \mathbf{q} = (x_d \ y_d \ z_d \ \delta e_{1d} \ \delta e_{2d} \ \delta e_{3d} \ x_f \ y_f \ z_f \ \delta e_{1f} \ \delta e_{2f} \ \delta e_{3f} \ x_m \ y_m \ z_m \ \delta e_{1m} \ \delta e_{2m} \ \delta e_{3m})^T$. $(\delta e_{1d} \ \delta e_{2d} \ \delta e_{3d})^T$, $(\delta e_{1f} \ \delta e_{2f} \ \delta e_{3f})^T$ and $(\delta e_{1m} \ \delta e_{2m} \ \delta e_{3m})^T$ are the Euler parameters of the rotation caused by the three types of errors respectively. Under a small deviation they are one-half of the Euler angles, i.e., $\delta e_1 = 0.5\alpha$, $\delta e_2 = 0.5\beta$, and $\delta e_3 = 0.5\gamma$. Parameters $(x_d y_d z_d \ \delta e_{1d} \ \delta e_{2d} \ \delta e_{3d})$ represent the transformation of surface due to the faulty setup with datum error, and $(x_f y_f z_f \ \delta e_{1f} \ \delta e_{2f} \ \delta e_{3f})$ represent the transformation due to the fixture error. $\boldsymbol{\varepsilon}_j$ is the noise term that corresponds to the j th feature. Using the variational approach proposed by Cai *et al.* (1997), we can find the relationship between parameters in $\delta \mathbf{q}$ and the error sources. This approach can be directly applied for the

fixture error, i.e.,

$$(x_f \ y_f \ z_f \ \delta e_{1f} \ \delta e_{2f} \ \delta e_{3f})^T = -\mathbf{J}^{-1} \boldsymbol{\Phi} \mathbf{E} \Delta \mathbf{f}, \quad (\text{A4})$$

where for generic workpiece, the Jacobian matrix \mathbf{J} is:

$$\mathbf{J} = \begin{pmatrix} -v_{1x} & -v_{1y} & -v_{1z} & 2(-f_{1z}v_{1y} + f_{1y}v_{1z}) & 2(f_{1z}v_{1x} - f_{1x}v_{1z}) & 2(-f_{1y}v_{1x} + f_{1x}v_{1y}) \\ -v_{1x} & -v_{1y} & -v_{1z} & 2(-f_{2z}v_{1y} + f_{2y}v_{1z}) & 2(f_{2z}v_{1x} - f_{2x}v_{1z}) & 2(-f_{2y}v_{1x} + f_{2x}v_{1y}) \\ -v_{1x} & -v_{1y} & -v_{1z} & 2(-f_{3z}v_{1y} + f_{3y}v_{1z}) & 2(f_{3z}v_{1x} - f_{3x}v_{1z}) & 2(-f_{3y}v_{1x} + f_{3x}v_{1y}) \\ -v_{11x} & -v_{11y} & -v_{11z} & 2(-f_{4z}v_{11y} + f_{4y}v_{11z}) & 2(f_{4z}v_{11x} - f_{4x}v_{11z}) & 2(-f_{4y}v_{11x} + f_{4x}v_{11y}) \\ -v_{11x} & -v_{11y} & -v_{11z} & 2(-f_{5z}v_{11y} + f_{5y}v_{11z}) & 2(f_{5z}v_{11x} - f_{5x}v_{11z}) & 2(-f_{5y}v_{11x} + f_{5x}v_{11y}) \\ -v_{11x} & -v_{11y} & -v_{11z} & 2(-f_{6z}v_{11y} + f_{6y}v_{11z}) & 2(f_{6z}v_{11x} - f_{6x}v_{11z}) & 2(-f_{6y}v_{11x} + f_{6x}v_{11y}) \end{pmatrix}. \quad (\text{A5})$$

$\mathbf{v}_j = (v_{jx} \ v_{jy} \ v_{jz})^T$ is the orientation vector of the datum planes $j = \text{I, II, and III}$. The Jacobian matrix is definitely full rank because the workpiece is deterministically located. The inverse of the Jacobian matrix therefore exists. Matrix $\boldsymbol{\Phi}$ is $\text{diag}(\mathbf{v}_I^T \mathbf{v}_I^T \ \mathbf{v}_I^T \mathbf{v}_I^T \ \mathbf{v}_I^T \mathbf{v}_I^T \ \mathbf{v}_{II}^T \mathbf{v}_{II}^T \ \mathbf{v}_{II}^T \mathbf{v}_{II}^T \ \mathbf{v}_{III}^T \mathbf{v}_{III}^T)$. \mathbf{E} is an 18×6 matrix, that is, $\text{diag}(\mathbf{E}_1 \ \mathbf{E}_1 \ \mathbf{E}_1 \ \mathbf{E}_2 \ \mathbf{E}_2 \ \mathbf{E}_3)$, where $\mathbf{E}_1 = (0 \ 0 \ 1)^T$, $\mathbf{E}_2 = (0 \ 1 \ 0)^T$, and $\mathbf{E}_3 = (1 \ 0 \ 0)^T$. We can also extend the variational approach for the EFE due to datum and machine tool errors, $\Delta \mathbf{d}$ and $\Delta \mathbf{m}$, respectively:

$$(x_d \ y_d \ z_d \ \alpha_d \ \beta_d \ \gamma_d)^T = -\mathbf{J}^{-1} \boldsymbol{\Phi} \mathbf{E} \Delta \mathbf{d}, \quad (\text{A6})$$

$$(x_m \ y_m \ z_m \ \alpha_m \ \beta_m \ \gamma_m)^T = -(-\mathbf{J}^{-1} \boldsymbol{\Phi} \mathbf{E} \Delta \mathbf{m}) = \mathbf{J}^{-1} \boldsymbol{\Phi} \mathbf{E} \Delta \mathbf{m}. \quad (\text{A7})$$

Equation (A7) has an additional minus sign due to the inverse transformation caused by the machine tool error transforming the workpiece from a nominal position to its real position. Combining Equations (A5), (A6), and (A9–A10), we get input matrix Γ_j corresponding to the machined surface j :

$$\Gamma_j = -\mathbf{A}_{jd} \mathbf{J}^{-1} \boldsymbol{\Phi} \mathbf{E}. \quad (\text{A8})$$

We can see that the matrices Γ_j corresponding to three EFEs are the same.

Biographies

Hui Wang received a B. Eng. degree in Mechanical Engineering from Shanghai Jiao Tong University, Shanghai, China in 2001, and an M.S.E. in Mechanical Engineering at the University of Michigan, Ann Arbor in 2003. He is currently a Ph.D. candidate in the Department of Industrial Management System Engineering at the University of South Florida, Tampa. His current research is on variation reduction for traditional and micro/nano scale manufacturing processes. He is a member of IIE and ASME.

Qiang Huang received B.S., M.S., and Ph.D. degrees in Mechanical Engineering from Shanghai Jiao Tong University, Shanghai, China in 1993, 1996, and 1998 respectively, and Ph.D. degree in Industrial and Operations Engineering at the University of Michigan, Ann Arbor. He is currently an assistant professor in the Department of Industrial Management System Engineering at the University of South Florida, Tampa. His research interests are centered on variation reduction for traditional and micro/nano scale manufacturing processes. He is a member of IIE, INFORMS, ASME, and SME.

Contributed by the Department